Journal of The Electrochemical Society, **157** (1) H31-H37 (2010)
0013-4651/2009/157(1)/H31/7/$28.00 © The Electrochemical Society

A Numerical Study of Thermal and Electrical Effects in a Vertical LED Chip

Farn-Shiun Hwu,[b] Jyh-Chen Chen,[a,z] Sheng-Han Tu,[c] Gwo-Jiun Sheu,[a] Hsueh-I Chen,[a] and Jinn-Kong Sheu[d]

[a]*Department of Mechanical Engineering and* [c]*Department of Optics and Photonics, National Central University, Jhongli City, Taoyuan 32001, Taiwan*
[b]*Department of Mechanical Engineering, Nanya Institute of Technology, Jhongli City, Taoyuan 32091, Taiwan*
[d]*Institute of Electro-Optical Science and Engineering and Center for Micro/Nano Science and Technology, National Cheng Kung University, Tainan 70101, Taiwan*

The influence of the size of an n-electrode and a current blocking layer (CBL) on the thermal and electrical characteristics of a vertical-injection GaN-based light emitting diode (LED) chip is investigated by numerical simulation. The predicted forward voltages are quite consistent with previous experimental data. The coupled thermal and electrical effects affect the performance of a LED chip. For cases without a CBL, the variation in current density and temperature distributions in the active layer, and the forward voltage and Joule heating percentage of the LED chip increase as the n-electrode width (L) decreases. The current crowding and temperature of the hot spot are very significant, although the wall-plug efficiency (WPE) is the highest one obtained for $L = 100$ μm. The better width of the n-electrode in terms of the uniformity of temperature, current density distribution, WPE, and forward voltage may be the case where $L = 200$ μm. The insertion of a CBL into a 600×600 μm chip leads to greater uniformity in the distribution of the current density in the effective light-emitting area when $L = 500$ μm. A more uniform temperature distribution in the active layer occurs when $L = 200$ μm, while the case when $L = 300$ μm has the maximum WPE.
 [DOI: 10.1149/1.3246784]

Manuscript submitted May 18, 2009; revised manuscript received September 15, 2009. Published November 3, 2009.

The vertical-injection GaN-based light emitting diode (LED) has demonstrated great potential for high power illumination usage.[1-4] The better current spreading and superior heat dissipation of the vertical LED make it able to operate under higher power conditions. The current distribution in the vertical-injection LED chip is usually estimated from the light output[1,2] and is affected by the size and pattern of the electrode, as well as the material properties of the chip.[1-4] A well-designed electrode pattern can result in a more uniform light output and better electrical characteristics.[2] Metallic substrates with enhanced heat dissipating ability have been used to improve the performance of vertical LEDs.[3] Better LED performance can also be achieved by lowering the resistivity of the transparent contact layer.[4] Current spreading in a lateral-injection LED can also be improved by the modification of the electrode pattern.[5-13] Several analytical models have been proposed to explain the current spreading phenomenon and possibly to obtain a better device geometry for LEDs.[5,6] Guo et al. improved the design by the incorporation of interdigitated mesh patterns for more uniform current spreading.[7] The current crowding effect can be reduced by the insertion of a current blocking layer (CBL) into p-electrodes for vertical LEDs [1] or under the p-electrode for lateral-injection LEDs.[8,9] The electrode pattern in LEDs has an influence on the voltage drop and light output power. Many different electrode patterns have been designed and fabricated in the search for a superior one that offers better performance.[10] However, this procedure is expensive and time-consuming. The construction of three-dimensional (3D) numerical simulation models to calculate the electric potential and current in the LED chip has proven to be much more economical.[11,12] Hwang and Shim[13] developed a 3D electrical circuit model to investigate the current spreading effect.

Most past studies have mainly been concerned with the effective light-emitting area and current crowding problem. Some have touched upon the influence of the thermal effect on the performance of LEDs, which has also affected the current distribution in the LED chip.[1-3,5,10,13] To explain the saturation of output power that occurs in experiments in small electrode areas, Kim et al.[1] conjectured that the output power may be degraded by an increased device resistance due to the thermal effect. The same argument about the impact of the thermal effect on output power has also been mentioned elsewhere.[2,3,13] The thermal effect can also degrade the lifetime of the LED device[5,14] and reduce the voltage drop across the contact and the junction.[10] The heat increases the junction temperature, decreases the luminous efficacy, shifts the point of chromaticity toward the blue end of the spectrum, decreases the color rendering index, and increases the color temperature.[14,15] From this, it can be seen that higher light output and lower heat generation are both critical concerns for the electrical-pattern design of LED chips. Joule heating and heat from nonradiative recombination effects are the two major sources of heat in high power LED chips.[3,5,10,13] The active layer is the dominant heat source at low current levels, where heat is created by nonradiative recombination. At high current levels, the contribution of Joule heating becomes increasingly important.[16] However, the size of the LED chip is so tiny that the temperature distribution in each layer is difficult to measure. Even now, most methods for measuring a chip temperature can obtain only the average temperature;[16,17] the thermal characteristics inside the LED chip are hard to observe. The local current density in each layer of the LED chip is also difficult to measure. Joule heating can be calculated by knowing the current distribution and the resistance of the device.[16] Recently, Bogdanov et al.[18] proposed a numerical model for simulating a conventional lateral-injection LED and an interdigitated multipixel array (IMPA) LED. They compared the results with their experiments. According to their hybrid approach, the IMPA LED avoids the current crowding effect, leading to much lower overheating in the active region.

In the present study, we modified the numerical model developed in our previous work[11,12] to include the thermal effect. We used this to investigate the thermal and electrical characteristics of vertical-injection LED chips operated under high power conditions. The effects of the n-electrode size and the CBL size were considered. The electrical pattern needed to achieve high wall-plug efficiency (WPE) is also discussed.

Numerical Model

A 600×600 μm vertical-injection LED chip is analyzed. A schematic representation of a cross section in the lateral direction is shown in Fig. 1. In the simulations, a quarter-symmetrical geometrical model was used to better represent the square shape of the LED chip.

[z] E-mail: jcchen@cc.ncu.edu.tw

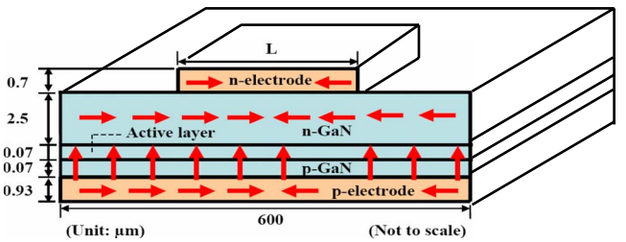

Figure 1. (Color online) A cross-sectional schematic representation of a vertical LED chip in the lateral direction, where L represents the size of the n-electrode.

The continuity equation for electronic transport in a LED is

$$\nabla \cdot (\sigma \nabla V) = 0 \quad [1]$$

where σ is the conductivity and V is the electrical potential. Except for the bottom boundary of the p-electrode and the top one of the n-electrode, the rest of the boundaries and the two symmetrical planes in the LED were all assumed to be insulated. The p-electrode was set to have a uniform input current density, and the n-electrode was set as the ground. Following our previous equivalent resistance method,[11,12] we simply assumed that the current flows through the active layer only in the vertical direction. As in our previous work,[11,12] the equation for calculating the electrical potential in the LED was solved using the finite-element method provided by the commercial program COMSOL Multiphysics. Each element in the active layer has an equivalent conductivity as proposed by

$$\sigma = \frac{l_e}{V_j} J_e \quad [2]$$

where l_e is the elemental thickness of the mesh, V_j is the voltage drop between the active layer, and J_e is the elemental current density. The J_e and V_j of each element satisfy the Shockley equation, which describes the current–voltage characteristics of the LED

$$J_e = J_0(\exp^{eV_j/nkT} - 1) \quad [3]$$

where J_0 is the saturation current density, n is the ideality factor, e is the elementary charge (1.6×10^{-19} C), k is the Boltzmann constant (1.38×10^{-23} J/K), and T is the absolute temperature. J_0 and n are dependent on the material quality and device structure. Nevertheless, J_0 is also affected by the temperature of the chip. The relationship can be described by[19]

$$J_0(T) = J_0|_{300\ K} \times 2^{(T-300)/10} \quad [4]$$

The same parameters were used for the geometric dimensions and for the Shockley equation as those used in previous studies;[1] i.e., the saturation current and n were set to be 4.72×10^{-22} A and 2.5, respectively. The thicknesses of the n-type GaN layer, the active layer, and the p-type GaN layer are 2.5, 0.07, and 0.07 μm, respectively. The resistivities of the n- and p-type cladding layers are $\rho_n = 1 \times 10^{-2}$ Ω cm and $\rho_p = 14$ Ω cm, respectively. The specific p-contact resistance and the specific n-contact resistance were set to be 2.8×10^{-3} and 3.6×10^{-4} Ω cm^2, respectively. The p-type electrode was formed by the application of a 0.93 μm thick Ag/Ni/Au metalized layer ($\rho_{Ag} = 1.59 \times 10^{-6}$ Ω cm/$\rho_{Ni} = 6.9 \times 10^{-6}$ Ω cm/$\rho_{Au} = 2 \times 10^{-6}$ Ω cm) on the entire wafer (600×600 μm). The n-type electrode was formed by a 0.7 μm thick Ti/Au metalized layer ($\rho_{Ti} = 4.2 \times 10^{-5}$ Ω cm) with various square dimensions and different widths (L = 100, 200, 300, 400, and 500 μm).

The steady-state equation for conduction heat transfer with the heat source is

Table I. Thermal conductivities used in the simulation.

Material	Ag	Ti	Ni	Au	SiO_2	GaN
k (W/m K)	374	17.1	55.2	290	1.38	120

$$-\nabla \cdot (k \nabla T) = \dot{q} \quad [5]$$

where k is the thermal conductivity. Based on the law of energy conservation, the input electrical power can be divided into two major parts; one is heat generation and the other is light output. Given the same assumption about active layers as in Eq. 2, we propose the heat generation term $\dot{q}$ in the active layer as follows

$$\dot{q} = J_e \times \left[V_j - \frac{\hbar\omega}{e} \times \eta_{int} \times \eta_{ext} \times \exp\left(- \frac{T - 300}{1600} \right) \right] / l_e \quad [6]$$

where $\hbar$ is the reduced Planck constant, ω is the angular frequency, η_{int} is the internal quantum efficiency at room temperature, and η_{ext} is the light extraction efficiency at room temperature. The term $\hbar\omega$ is the energy of the photon; thus, $(\hbar\omega/e)$ is the electrical potential converted from the energy of photon. Schubert[16] mentioned that the variation in the luminous intensity of a GaN LED with temperature is proportional to $\exp[-(T - 300)/1600]$. Therefore, the light output power per unit volume is assumed to be $J_e \times (\hbar\omega/e)\eta_{int} \times \eta_{ext} \times \exp[-(T - 300)/1600]/l_e$. The heat generated by light absorption inside the LED chip is assumed to be included in the $\dot{q}$ term. The values of the external quantum efficiency ($\eta_{int} \times \eta_{ext}$), as obtained in the literature,[18,20] are between 13 and 43%. Thus, in the present study, $\eta_{int} \times \eta_{ext} = 25\%$ was selected. The heat generation term per unit volume $\dot{q}$ due to Joule heating in the other layers of the LED chip is

$$\dot{q} = J_e \cdot \nabla V \quad [7]$$

The thermal conductivities of the materials are summarized in Table I.[18,21] The boundary conditions of the top, lateral, and bottom surfaces of the LED chip are shown by

$$\hat{n} \cdot (k \nabla T) = h_e(T_{inf} - T) \quad [8]$$

where $\hat{n}$ is the unit normal vector of the interface, T_{inf} is the air temperature, and h_e is the equivalent heat transfer coefficient. A copper slug with a board is usually used to dissipate the heat generated from the LED chip. The size was set to be about 7.2 cm^2 in the present study. Natural convection conditions affect the surfaces with $h_e = 5$ W/m^2 K, and T_{inf} is 300 K. Under the natural convection condition, the Biot number for the slug is very small; therefore, the temperature variation along the main heat flow direction inside the slug is insignificant. The convection from the bottom surface of the slug was replaced by the convection condition from the chip with the equivalent heat transfer coefficient h_e. For this case, h_e is about 40,000 W/m^2 K. The boundary condition of the symmetrical surfaces was set to be adiabatic and is shown by

$$\hat{n} \cdot (k \nabla T) = 0 \quad [9]$$

A self-developed code coupling the thermal and electrical equations was added to COMSOL Multiphysics to obtain the temperature, the electrical potential, and the current density in the LED chip. In the present study, the mesh for the epitaxial layer is made up of hexahedral elements, and that for the electrodes consists of the square-type ones. Convergence testing has been performed for element numbers with 3156, 6312, 9468, and 18,936. The relative tolerance was selected to be 1×10^{-6} for the temperature and voltage. The simulation results for temperature, current density, and voltage are almost the same for the cases of 9468 and 18,936. For this reason, and to save Central Processing Unit (CPU) time, the number of finite elements was chosen to be 9468 for the entire domain.

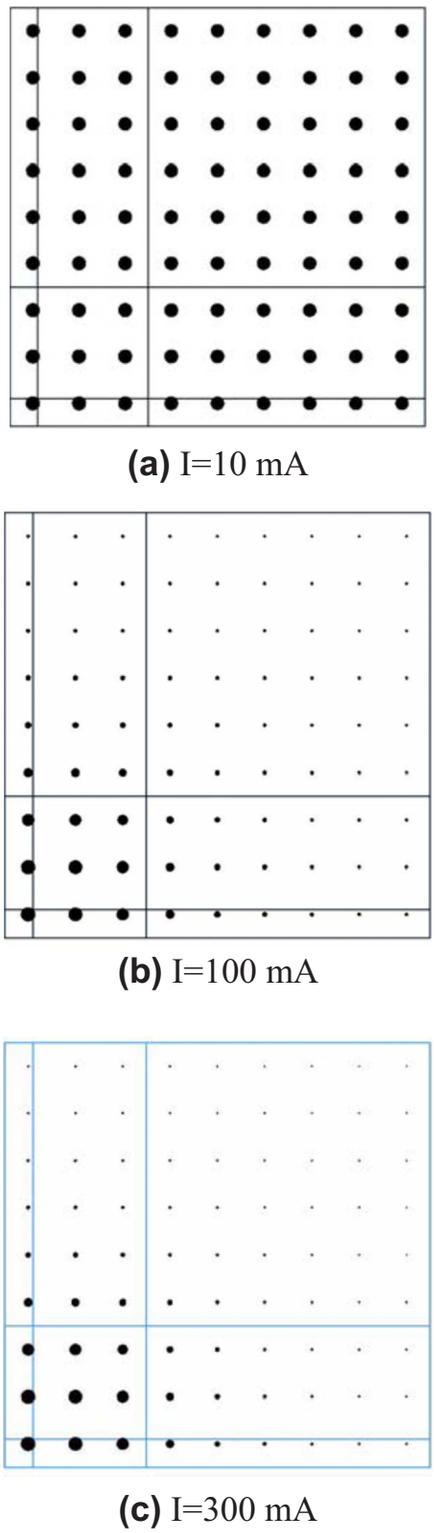

Figure 2. (Color online) Current densities (dot) on the active layer for different input currents.

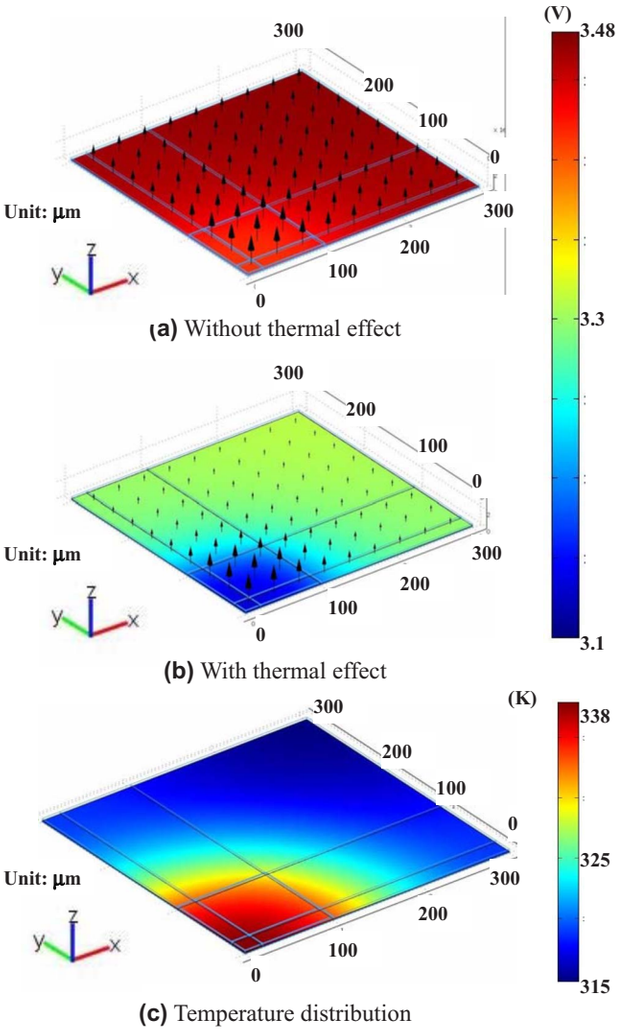

Figure 3. (Color online) [(a) and (b)] Electrical potentials (hue) and current densities (arrow) on the active layer for L = 200 μm; (c) temperature distribution for (b).

Results and Discussion

The vertical-injection LED is usually operated under high input power. Figure 2 displays the current densities in the active layer for different input currents for L = 200 μm without consideration of the thermal effect. Obviously, the crowding is significant when the input current is higher than 100 mA (the current density is about 27.8 A/cm^2). The current crowding is more serious beneath the n-electrode for higher operating current densities.

The results shown below are obtained when operated under an input current of 100 mA. Figure 3a and b shows the electric potentials (hue) and the current densities (arrows) in the active layer for L = 200 μm without and with the thermal effect, respectively. Figure 3c shows the temperature distribution for the case shown in Fig. 3b. The thermal and electrical effects coupled together influence the characteristics of the LED chip. Because current crowding appears in the center region, the highest temperature occurs at the center. The temperature decreases nearer to the edge due to the effects of Joule heating (Fig. 3c). Without the thermal effect, the electrical potential in the central region is smaller than that near the edge. The saturation current density (J_0) increases due to the higher temperature, while V_j decreases at fixed J_e when J_0 increases (Eq. 3). Hence, the electrical potential of the active layer is higher without consideration of the thermal effect (Fig. 3a) than with the thermal effect (Fig. 3b). Including the thermal effect, the discrepancy of the electrical potential between the central region and the edge becomes more significant (Fig. 3b), and the current crowding becomes more severe.

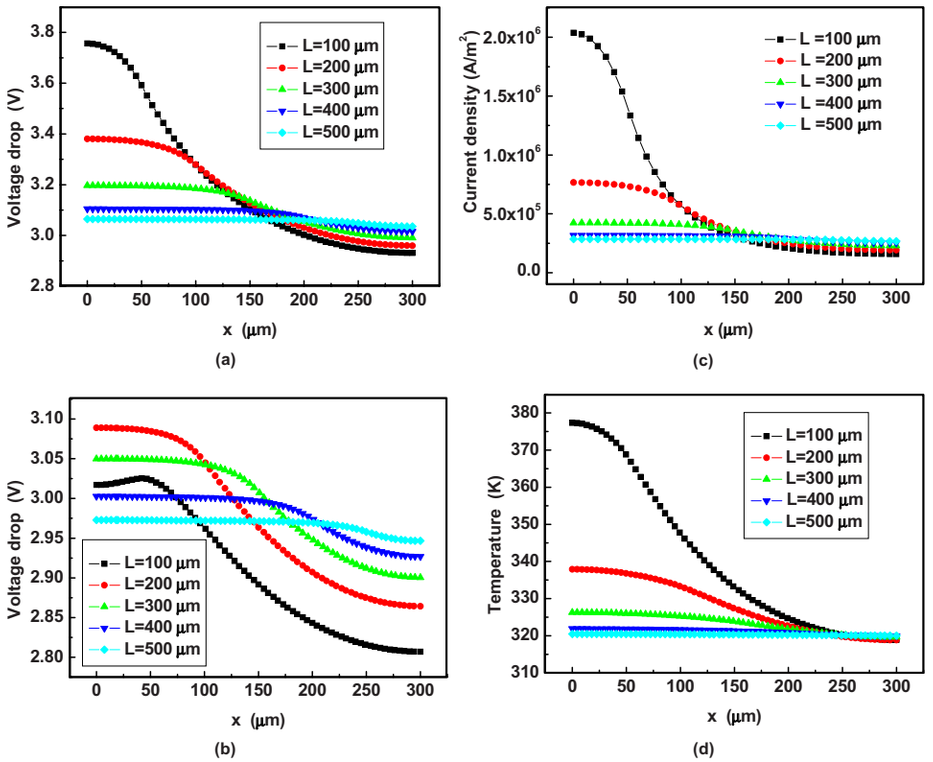

Figure 4. (Color online) Voltage drop across the active layer for the cases (a) without consideration of the thermal effect and (b) including the thermal effect, (c) current density distribution, and (d) temperature distribution from the center to the edge of the square, where x represents the distance from the center of the chip along the x-axis.

The voltage drop across the active layer from the center to the edge of the square (for different L), without and with the thermal effect, is illustrated in Fig. 4a and b, respectively. The distribution of current densities in the active layer, with the thermal effect, is shown in Fig. 4c, and the temperature distributions in the active layer are displayed in Fig. 4d. The origin is set as the center of the square. It can be seen in Fig. 4c that the current density distribution for L = 100 μm is similar to the light emission pattern obtained by Chu et al.[2] Due to the current crowding effect, when the width of the n-electrode is smaller, the uniformity of the current distribution in the active layer is worse (the difference between the maximum and minimum current densities is high) and the current crowds in the region under the n-electrode. However, light emission from this region is blocked by the n-electrode. Figure 4a and b shows that for L = 500 μm, the voltage drop across the active layer under the n-electrode is a little higher than that across the residual region of the active layer outside the area covered by the n-electrode. This phenomenon can be expected because the temperature is almost uniform at L = 500 μm (Fig. 4d). The temperature distribution for L = 500 μm is higher when the thermal effect is considered than when it is not. The voltage drop shifts from about 3.05 V (Fig. 4a) to about 2.96 V (Fig. 4b). A similar behavior is also shown when L = 400 μm. When the width of the n-electrode decreases, the voltage drop under the n-electrode is much higher than that in the active layer outside the region covered by the n-electrode for both L = 200 and 300 μm. This is because the current density under the n-electrode is much higher than that in the residual region of the active layer (Fig. 4c). The current crowding effect leads to a severe increase in temperature under the n-electrode. Because the voltage drop is degraded by the increase in temperature, the voltage drop for L = 200 μm is more obvious than that for L = 300 μm when the thermal effect is considered. The degradation in the voltage drop is smooth from the center to the edge under the n-electrode, but it decreases more significantly in the residual region of the active layer not covered by the n-electrode. In the cases where L is from 200 to 500 μm, the voltage drop across the active layer increases as the width of the n-electrode decreases. In contrast to L = 200–500 μm, when L = 100 μm, the voltage drop increases near the center of the active layer (x = 0) and decreases after the passing area covered by the n-electrode. It is smaller than that for L = 200 and 300 μm. The voltage drop is degraded by the increase in the temperature, but it is enhanced by the enlargement of the current density. The temperature around the center region of the active layer is very high for L = 100 μm (Fig. 4d), and the current crowding is very severe. The trend of the voltage to drop with x under the n-electrode for L = 100 μm may be due to the effect of the temperature being greater than that of the current crowding.

In Fig. 3b, it can be seen that there is current crowding under the n-electrode. The n-electrode obstructs light emitted from the top of the LED chip. This can be improved by installing a CBL to avoid the passage of current through the region under the n-electrode. As in Kim et al.,[1] the area of the CBL is set to be equal to the area of the n-electrode. The CBL is placed on the p-electrode, just under the n-electrode. Figure 5a-e shows the temperatures (hue) and current densities (arrow) in the active layer for different CBL (n-electrode) widths. Figure 6 reveals the distributions of current densities in the active layer from the center to the edge of the square for different L for the case with a CBL. As shown in Fig. 5, due to the existence of the nonconductive CBL in the p-electrode, the current densities almost disappear in the region beneath the n-electrode, and there is little growth near the region under the n-electrode. With the CBL, most of the current flows through the residual region of the active layer not covered by the n-electrode (effective light-emitting area). Therefore, the heat generation under n-electrode is significantly reduced, and the higher temperature region does not necessarily occur near the center of the active layer. This is very different from the cases without the CBL, where the maximum temperature appears at the center of the active layer. For L = 200 μm, the temperature distribution is more uniform (Fig. 5b). When L = 100 μm, the area of the CBL is still very small, only occupying 1/36 of the area of the p-electrode. There is significant current crowding in the region under the n-electrode (Fig. 5a and 6). This makes heat generation around the central region severe. The temperature is very high in the region under the n-electrode. The CBL has the effect of increasing

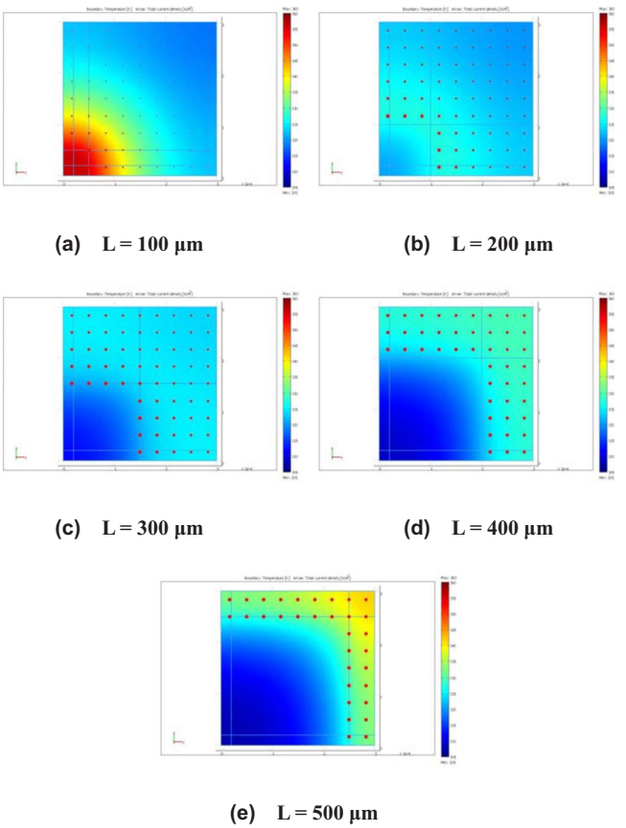

Figure 5. (Color online) Calculated temperatures (hue) and current densities (dot) in the active layer for five CBL (n-electrode) widths.

the local current density in the active layer outside the area covered by the n-electrode. This increases as the width of the CBL increases. However, there is still obvious current crowding in the region near the edge of the n-electrode in smaller L. A comparison of two cases with and without the CBL (Fig. 4c and 6) (L = 100 μm) is carried out to show the change in the uniformity of the current density. A comparison of Fig. 4c and 6 shows that the differences between the maximum and minimum current densities (ΔJ) are 1.88×10^6 and 7.22×10^5 A/m^2 for the cases without and with the CBL, respectively. Obviously, the current crowding effect can be significantly reduced by the CBL.

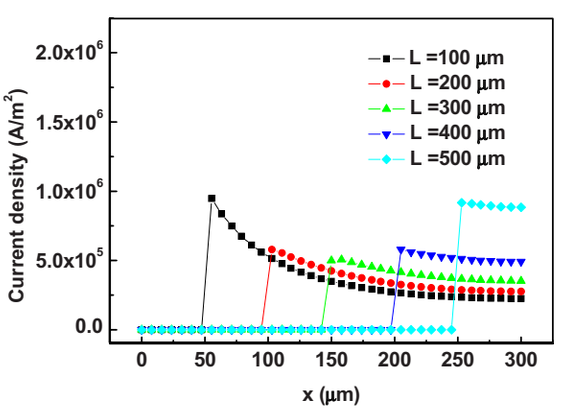

Figure 6. (Color online) Distribution of current density in the active layer from the center to the edge of the square for different L values for the case with CBL.

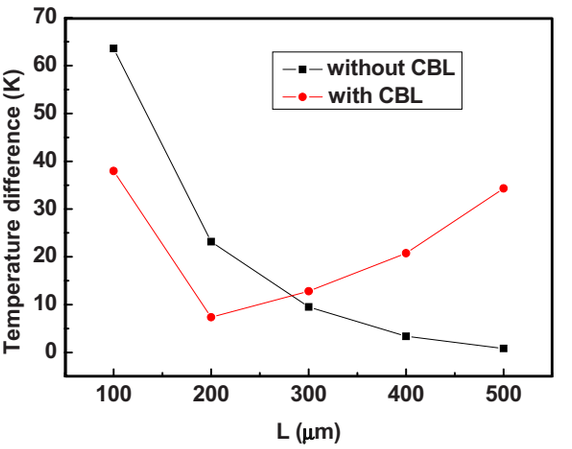

Figure 7. (Color online) Temperature differences in the active layer with different L values ranging from 100 to 500 μm for the cases with and without CBLs.

Figure 7 illustrates the differences between the maximum and minimum temperatures of the active layer for different n-electrode widths, with and without the CBL. As the n-electrode width increases, for the cases without CBL, the temperature difference (ΔT) in the active layer decreases because the current density distribution is more uniform for the larger n-electrode. However, the ΔT in the active layer increases as the width of the CBL increases for L = 300, 400, and 500 μm. The temperature in the central region is low, and that in the residual region of the active layer not covered by the n-electrode is high (Fig. 5c-e), because the current flows toward the residual region of the active layer due to the CBL effect. For L = 100 μm, the maximum temperature with the CBL shows a 40% decrease from that without the CBL. The current distribution is more uniform with the CBL (Fig. 6 and 4c). Therefore, the temperature distribution for L = 100 μm is more uniform, and the temperature difference is low. The addition of an appropriate CBL leads to a more uniform temperature distribution in the LED chip.

Figure 8 shows the forward voltages of the LED chip for different n-electrode widths for the cases with and without CBL. The numerical results are compared with the experimental data (without CBL) obtained by Kim et al.[1] The simulation results agree with their measurements. Because of the existence of the CBL, most current is forced to flow through the residual region of the active layer not covered by the n-electrode (Fig. 5), and the current flows through

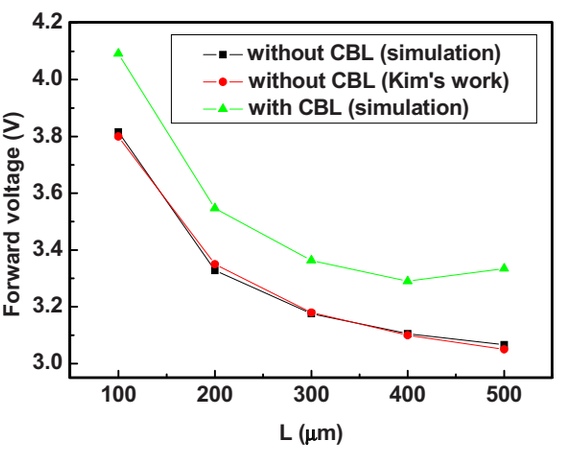

Figure 8. (Color online) Forward voltage with different L values ranging from 100 to 500 μm with and without CBL.

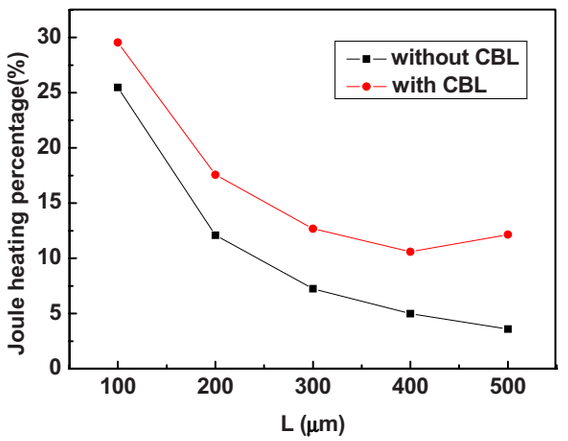

Figure 9. (Color online) Joule heating percentage with different L values ranging from 100 to 500 μm for the cases with and without CBL.

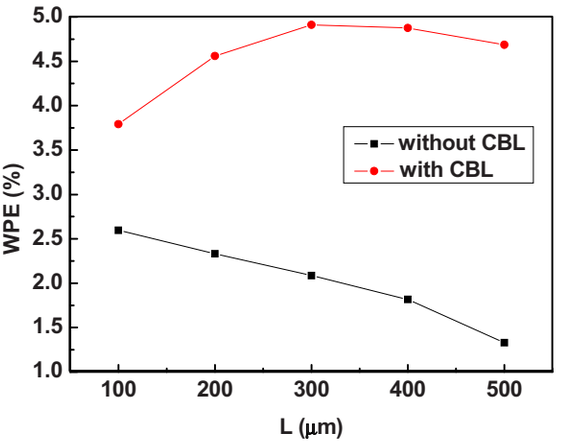

Figure 10. (Color online) Calculated WPE for different L values ranging from 100 to 500 μm for the cases with and without CBL.

the n-GaN layer in a lateral direction toward the n-electrode. The mean length of the current path for the case with the CBL is longer than that without the CBL, so the total resistance of the LED chip is larger and the forward voltage is also higher. In L = 100–400 μm, the forward voltages are reduced for larger widths of the n-electrode due to a lateral decrease in the resistance of the LED chip. However, the forward voltage is a little higher for L = 500 μm with the CBL than that for L = 400 μm. The forward voltage is degraded by an increase in the width of the n-electrode, but it is enhanced by the enlargement of the current density. The current density is much higher in L = 500 μm than in L = 400 μm (Fig. 6). Therefore, the increase in forward voltage for L = 500 μm with the CBL over that when L = 400 μm may be due to the much higher current density.

Figure 9 shows the relation of L to the Joule heating percentage of the total heat for the cases with and without CBLs. The width of the n-electrode has a big influence on the Joule heating generation, and the trend is similar to the forward voltage of the LED chip (Fig. 8, the lines indicated by squares and triangles) as the Joule heating in the LED chip can be calculated from the product of the current and the voltage drop in each layer, except the active layer. For the case with the CBL, the smallest percentage of Joule heating (10.6%) appears when L = 400 μm. With a further increase in L, the current crowding causes the Joule heating to increase. The contribution of Joule heating is more significant in the vertical LED chip when the n-electrode width decreases.

The WPE of the LED chip is defined as the output light power divided by the total input electrical power. Here, the output light power is selected as the electrical power generated by the residual region of the active layer not covered by the n-electrode subtracted from the total heat generated in the same region. Figure 10 illustrates the WPE for different n-electrode widths. The WPE for the case with the CBL is much higher (about 1.46–3.52 times) than that for the case without the CBL. This is because the current passes totally through the effective light-emitting area of the active layer for the case with the CBL, and the n-electrode obstructs light emission without the CBL. The trend of the variation in the WPE with the width of the n-electrode is very different for the two cases. Without the CBL, the WPE decreases as the width of the n-electrode increases because the proportion of the vertical current to the total electric current becomes larger. In contrast, with the CBL, the variation in the WPE increases with the width of the n-electrode, reaching the highest value when L = 300 μm, and then decreases. Based on the WPE results obtained in the present numerical simulation, the best width for the n-electrode (or the CBL) would be between 300 and 400 μm for the case with the CBL. Kim et al.[1] also measured the WPE for the cases with and without CBL, finding the WPE for the case with the CBL to be about 1.2 times that for the case without the CBL. Clearly, the present results are consistent with those of Kim et al. in that the WPE can be enhanced by the CBL.

Conclusion

In the present study, a numerical model is developed to investigate the coupling effect between the thermal and electrical characteristics in a vertical-injection GaN-based LED chip with a size of 600 × 600 μm. There is good agreement between the forward voltages predicted by the present computation taking into consideration the thermal effect and the experimental data measured by Kim et al.[1] The variation in voltage drop across the active layer and the current crowding are significantly enhanced by the temperature effect. The influences of the n-electrode size and the CBL size on the current density distribution, driving voltage, temperature distribution, Joule heating percentage, and WPE of LED chips are all investigated. For the cases without the CBL, the uniformity of temperature and current density distributions in the active layer gets worse, and the forward voltage and Joule heating percentage in the LED chip increase as the width of the n-electrode (L) decreases. When L = 100 μm, the current crowding ($\Delta J = 1.88 \times 10^6$ A/m^2) and temperature of the hot spot (ΔT = 63.6 K) are very significant, meaning that the high power vertical LED chip is poor, although the WPE (2.6%) is the highest one obtained. The case where L = 200 μm may have a better width of n-electrode in terms of the uniformity of temperature (ΔT = 23.2 K), current density distribution ($\Delta J = 5.74 \times 10^5$ A/m^2), WPE (2.33%), and forward voltage.

The advantages of inserting a CBL into a vertical LED are the following: It reduces temperature variation in the active layer (40%), improves the uniformity of the current density in the effective light-emitting area (61.6%), and increases the WPE of the LED chip (about 1.46–3.52 times). However, the disadvantage for inserting the CBL is that a higher input electrical power is required (the increment in forward voltage is 0.2–0.3 V), with the major portion of the input power being consumed by heat generation rather than light emitting. Under a fixed current, the maximum WPE (4.91%) appears in L = 300 μm. The temperature distribution in the active layer is more uniform (ΔT = 7.4 K) when L = 200 μm. The current density distribution in the effective light-emitting area is more uniform ($\Delta J = 3.3 \times 10^4$ A/m^2) when L = 500 μm.

Acknowledgment

The authors gratefully acknowledge the support of the National Science Council of Taiwan for this work through grant no. NSC 98-2221-E-008-100-MY3.

National Central University assisted in meeting the publication costs of this article.

References

1. H. Kim, K. K. Kim, K. K. Choi, H. Kim, J. O. Song, J. Cho, K. H. Baik, C. Sone, Y. Park, and T. Y. Seong, *Appl. Phys. Lett.*, **91**, 023510 (2007).
2. J. T. Chu, C. C. Kao, H. W. Huang, W. D. Liang, C. F. Chu, T. C. Lu, H. C. Kuo, and S. C. Wang, *Jpn. J. Appl. Phys., Part 1*, **44**, 7910 (2005).
3. S. J. Wang, K. M. Uang, S. L. Chen, Y. C. Yang, S. C. Chang, T. M. Chen, C. H. Chen, and B. W. Liou, *Appl. Phys. Lett.*, **87**, 011111 (2005).
4. D. W. Kim, H. Y. Lee, G. Y. Yeom, and Y. J. Sung, *J. Appl. Phys.*, **98**, 053102 (2005).
5. H. Kim, J. M. Lee, C. Huh, S. W. Kim, D. J. Kim, S. J. Park, and H. Hwang, *Appl. Phys. Lett.*, **77**, 1903 (2000).
6. H. Kim, S. J. Park, H. Hwang, and N. M. Park, *Appl. Phys. Lett.*, **81**, 1326 (2002).
7. X. Guo, Y. L. Li, and E. F. Schubert, *Appl. Phys. Lett.*, **79**, 1936 (2001).
8. S. J. Chang, C. F. Shen, W. S. Chen, T. K. Ko, C. T. Kuo, K. H. Yu, S. C. Shei, and Y. Z. Chiou, *Electrochem. Solid-State Lett.*, **10**, H175 (2007).
9. C. Huh, J. M. Lee, D. J. Kim, and S. J. Park, *J. Appl. Phys.*, **92**, 2248 (2002).
10. H. Kim, J. Cho, J. W. Lee, S. Yoon, H. Kim, C. Sone, Y. Park, and T. Y. Seong, *IEEE J. Quantum Electron.*, **43**, 625 (2007).
11. G. J. Sheu, F. S. Hwu, J. C. Chen, J. K. Sheu, and W. C. Lai, *J. Electrochem. Soc.*, **155**, H836 (2008).
12. J. C. Chen, G. J. Sheu, F. S. Hwu, H. I. Chen, J. K. Sheu, T. X. Lee, and C. C. Sun, *Opt. Rev.*, **16**, 213 (2009).
13. S. Hwang and J. Shim, *IEEE Trans. Electron Devices*, **55**, 1123 (2008).
14. N. Narendran, Y. Gu, J. P. Freyssinier, H. Yu, and L. Deng, *J. Cryst. Growth*, **268**, 449 (2004).
15. S. Chhajed, Y. Xi, Y. L. Li, Th. Gessmann, and E. F. Schubert, *J. Appl. Phys.*, **97**, 054506 (2005).
16. E. F. Schubert, *Light-Emitting Diodes*, 2nd ed., Cambridge University Press, Cambridge, U.K. (2006).
17. J. Kettle, R. M. Perks, and P. Dunstan, *Electron. Lett.*, **42**, 1122 (2006).
18. M. V. Bogdanov, K. A. Bulashevich, I. Y. Evstratov, A. I. Zhmakin, and S. Y. Karpov, *Semicond. Sci. Technol.*, **23**, 125023 (2008).
19. J. Millman and A. Grabel, *Microelectronics*, 2nd ed., McGraw-Hill, New York (1987).
20. K. Tadatomo, H. Okagawa, Y. Ohuchi, T. Tsunekawa, H. Kudo, Y. Sudo, M. Kato, and T. Taguchi, *Proc. SPIE*, **5187**, 243 (2004).
21. G. E. Myers, in *Analytical Methods in Conduction Heat Transfer*, 2nd ed., AMCHT, Madison, WI (1998).